Nature. Author manuscript; available in PMC 2010 May 13.

Published in final edited form as:
Nature. 2009 July 16; 460(7253): 410–413. doi:10.1038/nature08079.

Cohesins form chromosomal cis-interactions at the developmentally regulated *IFNG* locus

Suzana Hadjur[1], **Luke M Williams**[1], **Natalie K. Ryan**[1], **Bradley S Cobb**[1], **Tom Sexton**[2], **Peter Fraser**[2], **Amanda G Fisher**[1], and **Matthias Merkenschlager**[1]

[1]Lymphocyte Development Group, MRC Clinical Sciences Centre, Imperial College London, Du Cane Road, London W12 0NN, UK

[2]Laboratory of Chromatin and Gene Expression, The Babraham Institute, Cambridge CB2 4AT, UK

Abstract

Cohesin-mediated sister chromatid cohesion is essential for chromosome segregation and post-replicative DNA repair1,2. In addition, evidence from model organisms3-6 and from human genetics7 suggests that cohesin plays a role in the control of gene expression8,9. This non-canonical role has recently been rationalized by the findings that mammalian cohesin complexes are recruited to a subset of DNase I hypersensitive sites (HSS) and to conserved non-coding sequences by the DNA binding protein CTCF10-13. CTCF functions at insulators (which control interactions between enhancers and promoters) and at boundary elements (which demarcate regions of distinct chromatin structure)14, and cohesin contributes to CTCF's enhancer blocking activity10,11. The underlying mechanisms remain unknown, and the full spectrum of cohesin functions remains to be elucidated. Here we show that cohesin forms the topological and mechanistic basis for cell type-specific long-range chromosomal interactions *in cis* at the developmentally regulated cytokine locus *IFNG*. Hence, cohesin's ability to constrain chromosome topology is utilized not only for the purpose of sister chromatid cohesion1,2, but also to dynamically define the spatial conformation of specific loci. This novel aspect of cohesin function is likely of importance to normal development3-6 and to disease7.

One model of CTCF function is the formation of chromatin loops, which have been demonstrated at the *H19/IGF2*, beta globin and MHC class II loci15-17. Whether cohesin controls chromosome conformation is important for understanding its contribution to insulator and boundary element function18 and for elucidating the significance of cohesin binding to genomic locations unlikely to constitute insulators or chromatin boundaries, including sites within the coding regions of active genes10,11.

Cohesin binding within a developmentally regulated gene is exemplified by *IFNG*, which encodes the cytokine interferon-γ (Ifn-γ). A conserved cohesin site is located within the first intron of the mouse *Ifng* and the human *IFNG* coding region10. The *Ifng* locus harbors numerous conserved non-coding sequences and putative cis-regulatory elements that are located at considerable distances from the coding region19-21 and can function as enhancers or insulators20. Genomic tiling arrays10 showed major binding sites for the cohesin subunit Rad21 and CTCF at −73 and +66 kb in mouse lymphoid cell lines (figure 1a). ChIP and real time PCR analysis of the human 293T cell line and of primary CD4 T cells sorted from human peripheral blood demonstrated strong binding of cohesin and CTCF at orthologous

Address correspondence to matthias.merkenschlager@csc.mrc.ac.uk, Tel + 44 208 383 8239.

The authors have no financial conflicts of interest.

Europe PMC Funders Author Manuscripts

sequences located 63 kb upstream of *IFNG* and at evolutionary conserved regions (ECR, www.decode.org) at +1.5 and +119 kb in the human *IFNG* region (figure 1b, see legend for details). Analysis of genome-wide ChIP-sequencing data22 confirmed −63, +1.5 and +119 kb as the major CTCF sites in human CD4 T cells and showed that features of canonical CTCF sites, namely the histone H2A variant H2AZ and trimethylated histone H3 lysine-4 (H3K4me3) were present at −63 and +1.5 kb (not shown).

Naive, non-polarized CD4 T cells are the progenitors of specialized T helper (Th) cell types, including Th1 cells (which confer immunity to intracellular pathogens) and Th2 cells (which aid antibody production and mediate responses to helminths). Th cell differentiation has become a paradigm for how genetically identical cells acquire distinct gene expression programs by the interplay of transcription factors and chromatin regulators23. The *IFNG* locus is prepared for expression during the differentiation of Th1 cells: DNA methylation declines20,24, cell type-specific HSS emerge19-21 and *IFNG* transcription becomes inducible23. Conversely, *IFNG* is silenced during Th2 differentiation23. To gain insight into the developmental regulation of cohesin and CTCF at human *IFNG* we isolated Th1 and Th2 effector memory cells (figure 1c). These cells arise *in vivo*, can be identified based on the expression of the chemokine receptor CCR5 and the prostaglandin D2 receptor CRTh2, respectively25, and retain their cytokine profiles when expanded *in vitro* under non-polarising conditions25. Real time RT-PCR showed that *IFNG* transcripts were highly induced upon activation of $CCR5^+$ Th1 cells (figure 1c) and intracellular staining showed the inducible expression of IFNγ protein in $CCR5^+$ Th1 cells, while $CRTH2^+$ Th2 cells expressed interleukin-4 (IL4, figure 1c). The positioning of CTCF and cohesin binding sites across *IFNG* was similar between non-polarized CD4 T cells, $CCR5^+$ Th1 cells, $CRTH2^+$ Th2 cells and non-lymphoid 293T cells (figure 1b), consistent with the reported preference of CTCF and cohesin for constitutive HSS10. Interestingly, however, both cohesin and CTCF were significantly more abundant at the −63, +1.5 and +119 kb sites in $CCR5^+$ Th1 cells (figure 1b). Increased cohesin and CTCF binding in $CCR5^+$ Th1 cells was selective for the *IFNG* locus, since $CCR5^+$ Th1 and $CRTH2^+$ Th2 cells expressed similar levels of Rad21 and CTCF (supplementary figure 1a), and the occupancy of control sites outside the *IFNG* region was equivalent (supplementary figure 1b).

Analysis of activating and repressive post-translational histone modifications across the *IFNG* region suggested boundary element function for the −63 site, but not the +1.5 or the +119 kb sites in non-polarised human CD4 T cells26. We therefore explored whether these sites have additional functions in organising the *IFNG* region in 3-dimensional nuclear space by chromosome conformation capture27 (3C) experiments on $CCR5^+$ Th1 and $CRTH2^+$ Th2 chromatin templates (supplementary figure 2). The inducible nature of *IFNG* expression in $CCR5^+$ Th1 cells allowed us to define the chromosome topology of the locus in its inducible state from changes in locus conformation that may accompany high-level transcription. Using a Hind III restriction fragment harboring the intronic +1.5 kb site as a bait, we looked for long-range interactions with sites across the *IFNG* genomic region. Crosslinking frequencies fell with increasing distance from the bait, but were significantly increased for the CTCF and cohesin sites at −63 and +119 kb, indicating long-range interactions at *IFNG* that occur selectively in $CCR5^+$ Th1 cells (figure 2a). Nuclear dimensions were similar for $CCR5^+$ Th1 and $CRTH2^+$ Th2 cells (figure 2b), which rules out spatial constraints as an explanation for increased crosslinking efficiencies in $CCR5^+$ Th1 cells. Since the *IFNG* loci on homologous chromosomes were separated by at least 1.5 μm in 3-dimensional fluorescence in situ hybridisation (3D FISH) experiments (figure 2b) and long-range interactions in the *IFNG* genomic region were readily detectable in purified G_1 cells (i.e. prior to DNA replication and the formation of sister chromatids, figure 2c), the interactions recorded by 3C most likely occurred in *cis*, not in *trans* between *IFNG* alleles. These data establish that CTCF and cohesin sites form the topological basis for cell type-

specific, long-range interactions at *IFNG* that occur preferentially in human CCR5$^+$ Th1 cells.

We next explored the relationship of CTCF and cohesin with long-range chromosomal interactions. Depletion of CTCF by siRNA-mediated knockdown in CCR5$^+$ Th1 cells resulted in reduced 3C interactions between the *IFNG* locus (+1,5 kb) and the −63 and +119 kb sites (supplementary figure 4), reminiscent of the role for CTCF in long-range interactions at other loci15-17. Importantly, Rad21 knockdown substantially reduced long-range interactions of the *IFNG* coding region with the −63 and the +119 kb sites (figure 3a), demonstrating that the conformation of the locus depended on cohesin as well as CTCF. ChIP analysis of the IFNG region in CCR5$^+$ Th1 cells showed that Rad21 RNAi reduced the binding of Rad21 to its sites at *IFNG*, while CTCF remained bound (figure 3b). This result suggests that CTCF cannot maintain long-range interactions at *IFNG* in the absence of cohesin. Control experiments established that Rad21 knockdown did not interfere with technical aspects of the 3C methodology (supplementary figure 2) or with cell cycle progression of human CCR5$^+$ Th1 cells (supplementary figure 5). Interestingly, basal *INFG* transcript levels were reduced by half (50±13%, n=5, $p<0.005$, one sided T test) in Rad21 depleted CCR5$^+$ Th1 cells (figure 3c) and the inducibility of *INFG* transcripts upon T cell activation was reduced to 76±12% of control levels (figure 3c, n=4, $p<0.05$). These effects were selective since the inducibility of *IL2* was not compromised (115±30%, n=3) and the expression of *IGF2*, which is restricted to the paternal allele by cohesin11, was elevated (247±148%, n=3, $p<0.05$) in Rad21 depleted CCR5$^+$ Th1 cells (figure 3c). The basal and inducible expression of IFNγ protein were also reduced (to 48±9%, n=4, $p<0.05$ and 57±7%, n=4, $p<0.05$) by Rad21 knockdown (figure 3c). Hence, cohesin is required for the CCR5$^+$ Th1 cell-specific conformation of the *IFNG* locus and contributes to its regulation.

Taken together, these data show that the remodelling of the developmentally regulated *IFNG* locus during the differentiation of naive CD4 T cells into Th1 cells is accompanied by the enhanced association of CTCF and cohesin with a select set of conserved sequence elements. CTCF and cohesin - perhaps in collaboration with other factors or modifications - mediate Th1-specific long-range interactions between these sites. Recent data provide support for an ‘architectural role’ of CTCF/cohesin sites in chromosome conformation28. Our data show that long-range interactions mediated by cohesin can be dynamically regulated in a developmental context, rather than static in nature. An attractive scenario is that CTCF recruits cohesins to specific sites10-13, and that cohesins in turn mediate chromosomal interactions between these sites *in cis* (this study). This novel aspect of cohesin function is likely to be of general importance in defining local and global genome topology. Cohesin-mediated chromosomal *cis*-interactions provide one possible mechanism for the impact of cohesin on the regulation of H19/Igf2 (reference 11, 9, and J-M Peters and A Murrell, personal communication), of cytokine loci such as *IL4, IL5, IL13* and *Ifng29*, MHC class II genes17 and of other loci9,11 that depend on CTCF/cohesin for their appropriate expression. We speculate that by constraining the physical conformation of chromatin, cohesin may affect the probability with which gene regulatory elements interact with each other, both negatively and positively, in normal development3-7 and in disease7.

Supplementary Material

Refer to Web version on PubMed Central for supplementary material.

Acknowledgments

We thank Drs. Mara Messi, Federica Sallusto and Ludovica Bruno for help and advice with human T cells, Dr. Luis Aragon for discussions, Drs. Marion Leleu and Mikhail Spivakov for help with informatics, Dr. Dirk Dormann for

help with image analysis and Eugene Ng, Eric O'Connor and Dr Phil Hexley for cell sorting. Supported by the Medical Research Council, UK.

APPENDIX

Methods summary

Naive human CD4 T cells, $CCR5^+$ Th1 and $CRTh2^+$ Th2 effector memory cells were isolated by flow cytometry as described25. ChIP and real time PCR, RNA isolation, RT-PCR, siRNA transfection (Amaxa) and immunoblotting have been described10. As detailed in supplementary information, human T cells were mixed 5:1 with mouse B3 pre-B cells10, fixed, and isolated nuclei were digested with HindIII at >80% efficiency at each HindIII site tested. Religated restriction fragments were assayed by TaqMan PCR using custom dual-labelled fluorogenic probes (Sigma). 3C primers for mouse *Acta2*, human *ACTA2* and *IFNG* were designed and tested as detailed in supplementary figure 2. Data were normalized to mouse *Acta2* or human *ACTA2* as indicated. 3D-FISH and distance measurements with Volocity software (Perkin-Elmer/Improvision) have been described30.

Materials and methods

Cell sorting and culture

The use of human cells was approved by the local National Health Service Trust Research Ethics Committee. CD4 T cells were enriched with CD4 microbeads (Miltenyi Biotech). Naive $CD4^+$ $CD45RA^+$ (ImmunoTech, Beckman Coulter) and $CCR5^+$ Th1 (anti-CCR5, BD Biosciences) or $CRTh2^+$ Th2 (anti-CD294, Miltenyi Biotech) effector memory cells were isolated by flow cytometry, activated with plate bound anti-CD3 and anti-CD28 for 4 days and expanded in media containing IL2 as described25. Naive cells were maintained in a non-polarized state by addition of anti-IL4 and anti-IL12 (eBiosciences). Cytokine expression was induced with plate bound anti-CD3 and anti-CD28 and evaluated by intracellular staining, real time RT-PCR or ELISA (IFNγ Quantikine, R&D Systems).

Real time RT-PCR

RNA was isolated using RNAbee (Tel-Test, Friendswood, TX) and reverse transcribed. PCR reactions included 2x SYBR PCR Master Mix (Qiagen), 300nM primers and 2 μl of cDNA as a template in 50μl reaction volume. Cycle conditions were 94° C for 8 min, 40 cycles of 94° C for 30 sec, 55° C for 30 sec, 72° C for 1 min, followed by plate read. All primers amplified specific cDNAs with at least 95% efficiency. Data were normalized against the average of three housekeeping genes, *GAPDH, HPRT* and *TBP*. Primer sequences were (5′ to 3′):

GAPDH fw TCTGCTCCTCCTGTTCGACA rev AAAAGCAGCCCTGGTGACC

HPRT fw TCCTTGGTCAGGCAGTATAATCC rev GTCAAGGGCATATCCTACAACAAA

TBP fw CCGGCTGTTTAACTTCGCTT rev TTTTCCTAGAGCATCTCCAGCAC

IFNG fw GTTTTGGGTTCTCTTGGCTGTTA rev ATTATCCGCTACATCTGAATGACCT

IL4 fw GCGATATCACCTTACAGGAGATCA rev GTGTTCTTGGAGGCAGCAAAG

IL2 fw AACACAGCTACAACTGGAGCATTT rev AAATGTGAGCATCCTGGTGAGTTT

Europe PMC Funders Author Manuscripts

IGF2 fw ACACCCTCCAGTTCGTCTGT rev CGGAAACAGCACTCCTCAAC

CTCF fw GGGGAAAATGGAGGAGAAAC rev GCTCCTCCTCATCCTCATTG

RAD21 fw TGACTTTGATCAGCCACTGC rev RT TCCCAACTTCTTCTCTCATGG

Chromatin immunoprecipitation

Formaldehyde (1%) was added to the culture medium at room temperature, blocked after 10 minutes with 0.125M glycine, and cells were washed in cold PBS. Nuclear extracts were prepared and pellets were lyzed in 150 mM NaCl, 25 mM Tris-HCl (pH 7.5), 5 mM EDTA, 1% Triton X, 0.1% SDS, 0.5% deoxycholate for 30min on ice. Chromatin was sonicated to an average fragment size of 500 bp, centrifuged to pellet debris, incubated at 4°C with BSA- and salmon sperm-blocked magnetic PGS beads (Dynal) for 2 h and then overnight with PGS beads coated with rabbit anti-Rad21 (Abcam) or rabbit anti-CTCF (Upstate Biotech). The beads were sequentially washed for 5 min with low-salt buffer (0.1% SDS, 1% TritonX, 2 mM EDTA, 20 mM Tris-HCl, 150 mM NaCl), high-salt buffer (0.1% SDS, 1% TritonX, 2 mM EDTA, 20 mM Tris-HCl, 500 mM NaCl) and LiCl buffer (0.25 M LiCl, 1% NP-40, 1% deoxycholate, 1 mM EDTA, 10 mM Tris-HCl). Chromatin was RNase treated and extracted in elution buffer (1% SDS, 0.1 M $NaHCO_3$). DNA cross-links were reversed at 65°C over night, samples were phenol-chloroform extracted and assessed by real-time PCR.

siRNA transfection and chromosome conformation capture

Human T cells were electroporated (Amaxa) with siRNA oligonucleotides and siGLO-PE transfection indicator (Dharmacon) or siGLO-PE alone using the Amaxa human T cell Nucleofector kit according to the protocol provided by the manufacturer (Amaxa Biosystems). Viable siGLO-PE positive cells were isolated by cell sorting and used for ChIP or 3C experiments. For 3C, 10^7 human T cells were mixed with 2×10^6 mouse B3 pre-B cells5. Formaldehyde (1%) was added to the culture medium at room temperature, blocked after 10 minutes with 0.125M glycine, and the cells were washed with cold PBS before lysis in 10mM Tris (pH 7.5), 10mM NaCl, 5mM $MgCl_2$, 0.2% NP40 for 20min on ice. Nuclei were washed and agitated at 37°C for 1hr in 500μl of 1.2x NEB Buffer 2 with 0.3% SDS and for 1h in 1.2x NEB Buffer 2 with 2% TritonX and over night with 1500 units HindIII followed by 30min at 65°C in 1.5% SDS. Samples were diluted into 1.1x T4 DNA ligase buffer (NEB) containing 1% TritonX and incubated at 37°C for 1 hr. T4 DNA ligase was added (800 units) at 16°C for 4h. Cross-links were reversed at 65°C over night and DNA was purified by phenol-chloroform extraction. Real-time PCR was performed in triplicate using TaqMan master mix (Qiagen) and custom dual-labelled fluorogenic probes (Sigma). 3C primers for human *ACTA2* and *IFNG* as well as mouse *Acta2* were designed and tested as detailed in supplementary figure 2 and 3C data were normalized to mouse *Acta2* or to human *ACTA2* as indicated. For 3C analysis of cells in the G_1 phase of the cell cycle cells were fixed as described above and stained with 50 μg/ml propidium iodide in the presence of 0.05% NP40 and 1.5 mg/ml RNaseA for 1hr at room temperature and G_1 cells were sorted by flow cytometry. Control cells were left unsorted.

3D-FISH and distance measurements with Volocity software (Perkin-Elmer/Improvision) were done as described30 using the *IFNG* BAC CTD2532A1 as a probe.

References

1. Nasmyth K, Haering CH. The structure and function of SMC and kleisin complexes. Annu Rev Biochem. 2005; 74:595–648. [PubMed: 15952899]
2. Hirano T. At the heart of the chromosome: SMC proteins in action. Nat Rev Mol Cell Biol. 2006; 7:311–322. [PubMed: 16633335]

3. Horsfield JA, et al. Cohesin-dependent regulation of Runx genes. Development. 2007; 134:2639–2649. [PubMed: 17567667]
4. Pauli A, et al. Cell-type-specific TEV protease cleavage reveals cohesin functions in Drosophila neurons. Dev. Cell. 2008; 14:239–251. [PubMed: 18267092]
5. Schuldiner O, et al. piggyBac-based mosaic screen identifies a postmitotic function for cohesin in regulating developmental axon pruning. Dev. Cell. 2008; 14:227–238. [PubMed: 18267091]
6. Zhang B, et al. Mice lacking sister chromatid cohesion protein PDS5B exhibit developmental abnormalities reminiscent of Cornelia de Lange syndrome. Development. 2007; 134:3191–3201. [PubMed: 17652350]
7. Liu J, Krantz ID. Cohesin and human disease. Annu Rev Genomics Hum Genet. 2008; 9:303–320. [PubMed: 18767966]
8. Hagstrom KA, Meyer BJ. Condensin and cohesin: more than chromosome compactor and glue. Nat Rev Genet. 2003; 4:520–534. [PubMed: 12838344]
9. Dorsett D. Roles of the sister chromatid cohesion apparatus in gene expression, development, and human syndromes. Chromosoma. 2007; 116:1–13. [PubMed: 16819604]
10. Parelho V, et al. Cohesins functionally associate with CTCF on mammalian chromosome arms. Cell. 2008; 132:422–433. [PubMed: 18237772]
11. Wendt KS, et al. Cohesin mediates transcriptional insulation by CCCTC-binding factor. Nature. 2008; 451:796–801. [PubMed: 18235444]
12. Stedman W, et al. Cohesins localize with CTCF at the KSHV latency control region and at cellular c-myc and H19/Igf2 insulators. EMBO J. 2008; 27:654–666. [PubMed: 18219272]
13. Rubio ED, et al. CTCF physically links cohesin to chromatin. Proc Natl Acad Sci USA. 2008; 105:8309–8314. [PubMed: 18550811]
14. Wallace JA, Felsenfeld G. We gather together: insulators and genome organization. Curr Opin Genet Dev. 2007; 17:400–407. [PubMed: 17913488]
15. Kurukuti S, et al. CTCF binding at the H19 imprinting control region mediates maternally inherited higher-order chromatin conformation to restrict enhancer access to Igf2. Proc Natl Acad Sci USA. 2006; 103:10684–10689. [PubMed: 16815976]
16. Splinter E, et al. CTCF mediates long-range chromatin looping and local histone modification in the beta-globin locus. Genes Dev. 2006; 20:2349–2354. [PubMed: 16951251]
17. Majumder P, Gomez JA, Chadwick BP, Boss JM. The insulator factor CTCF controls MHC class II gene expression and is required for the formation of long-distance chromatin interactions. J. Exp. Med. 2008; 205:785–798. [PubMed: 18347100]
18. Gause M, Schaaf CA, Dorsett D. Cohesin and CTCF: cooperating to control chromosome conformation? Bioessays. 2008; 30:715–718. [PubMed: 18623068]
19. Lee DU, Avni O, Chen L, Rao A. A distal enhancer in the interferon-gamma locus revealed by genome sequence comparison. J Biol Chem. 2004; 279:4802–4810. [PubMed: 14607827]
20. Schoenborn JR, et al. Comprehensive epigenetic profiling identifies multiple distal regulatory elements directing transcription of the gene encoding interferon-gamma. Nat. Immunol. 2007; 8:732–742. [PubMed: 17546033]
21. Hatton RD, et al. A distal conserved sequence element controls *Ifng* gene expression by T cell and NK cells. Immunity. 2008; 25:717–729. [PubMed: 17070076]
22. Barski A, et al. High-resolution profiling of histone methylations in the human genome. Cell. 2007; 129:823–837. [PubMed: 17512414]
23. Ansel KM, Lee DU, Rao A. An epigenetic view of helper T cell differentiation. Nat Immunol. 2003; 4:616–623. [PubMed: 12830136]
24. Jones B, Chen J. Inhibition of IFN-gamma transcription by site-specific methylation during T helper cell development. EMBO J. 2008; 25:2443–2452. [PubMed: 16724115]
25. Messi M, et al. Memory and flexibility of cytokine gene expression as separable properties of human T(H)1 and T(H)2 lymphocytes. Nat Immunol. 2003; 4:78–86. [PubMed: 12447360]
26. Cuddapah S, Jothi R, Schones DE, Roh TY, Cui K, Zhao K. Global analysis of the insulator binding protein CTCF in chromatin barrier regions reveals demarcation of active and repressive domains. Genome Res. 2009; 19:24–32. [PubMed: 19056695]

27. Dekker J. The three ‘C’ s of chromosome conformation capture: controls, controls, controls. Nat Methods. 2006; 3:17–21. [PubMed: 16369547]

28. Mishiro T, Ishihara K, Hino S, Tsutsumi S, Aburatani H, Shirahige K, Kinoshita Y, Nakao M. Architectural roles of multiple chromatin insulators at the human apolipoprotein gene cluster. EMBO J. Mar 26.2009 epub.

29. Ribeiro de Almeida C, et al. Critical role for the transcription regulator CCCTC-binding factor in the control of Th2 cytokine expression. J Immunol. 2009; 182:999–1010. [PubMed: 19124743]

30. Hewitt SL, High FA, Reiner SL, Fisher AG, Merkenschlager M. Nuclear repositioning marks the selective exclusion of lineage-inappropriate transcription factor loci during T helper cell differentiation. Eur. J. Immunol. 2004; 34:3604–3613. [PubMed: 15484194]

Europe PMC Funders Author Manuscripts

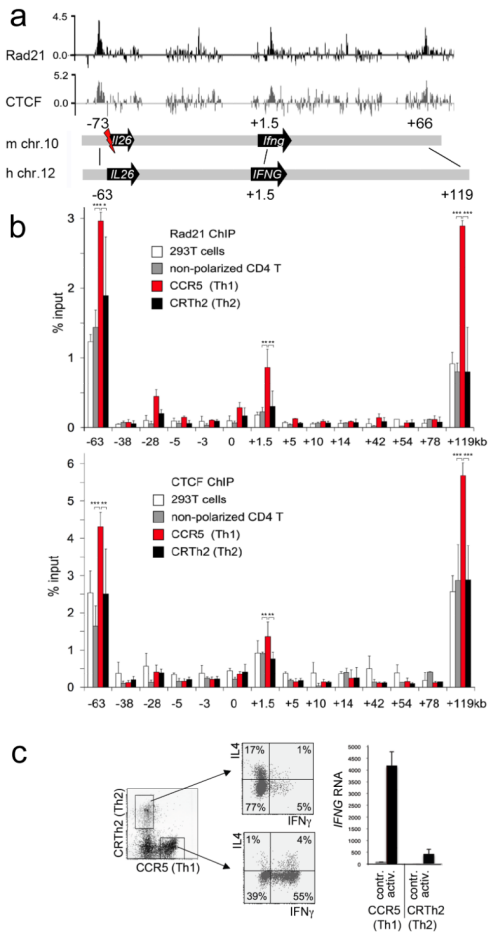

Figure 1. Developmentally regulated cohesin and CTCF binding at *IFNG*

a) ChIP and genomic tiling array data for the mouse B3 pre-B cell line10 show log2 enrichment of the cohesin subunit Rad21 (black) and CTCF (gray) at *Ifng*. Schematic representation of the mouse *Ifng* region (m chr.10) and the human *IFNG* region (h Chr.12), a flash indicates genomic rearrangement at *Il26*, a pseudogene in rodents20.

b) ChIP and real time PCR mapping of Rad21 (top) and CTCF (bottom) at human *IFNG* in 293T cells (white), non-polarized CD4 T cells (grey), CCR5$^+$ Th1 (red) and CRTh2$^+$ Th2 (black) effector memory cells. Star symbols indicate statistical significance (Student's T test) *** p<0.005, ** p<0.05, * p<0.05. Primer positions are indicated relative to the *IFNG* transcription start site. Human/mouse identity at the −63 kb site is 59% over 291bp surrounding a canonical CTCF consensus motif. Two evolutionary conserved regions (ECR, www.dcode.org) are found at +1.5 kb (70.2% and 69.1% identity over 104 and 217bp) and three at +119 kb (70.0%, 71.0% and 62.2 and 69,1% identity over 120, 100 and 45bp). Positive control sites at Chr11:118283kb, Chr11:118333kb, *CD8* Cluster I and *ZPF54* were included in all experiments (supplementary figure 1) and data are normalized to Chr11:118283kb (mean±SD, n=4).

c) Isolation (left) of human effector memory CCR5$^+$ Th1 and CRTh2$^+$ Th2 cells and cytokine expression assessed by intracellular staining and flow cytometry (middle) or real time RT-PCR analysis before (contr.) and after activation with plate bound anti-CD3 and anti-CD28 (activ., right).

Europe PMC Funders Author Manuscripts

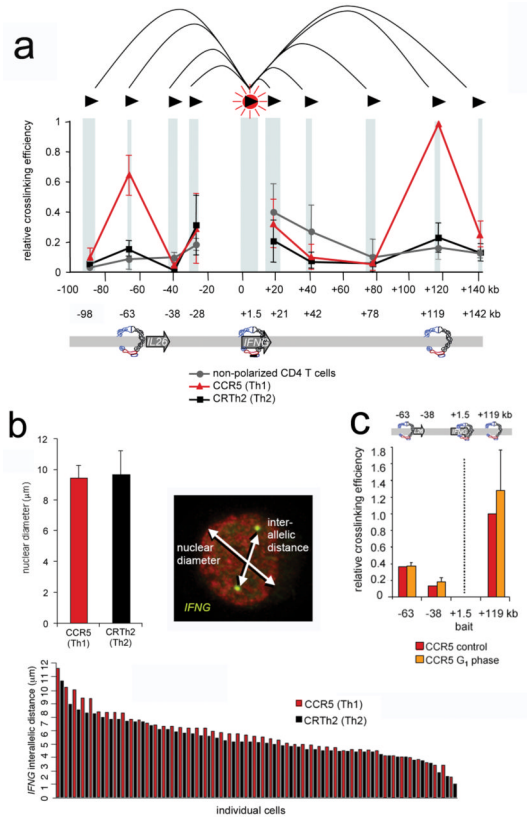

Figure 2. Cell type-specific long-range chromosomal interactions at *IFNG* are based on CTCF/cohesin sites

a) Chromosome conformation capture (3C) and Taqman PCR were used to determine interactions between *IFNG* +1.5 kb (beacon) and primers (black arrowheads) placed within the indicated HindIII fragments (shaded blue) in non-polarized CD4 T cells (grey), CCR5$^+$ Th1 (red) and CRTh2$^+$ Th2 (black) cells (supplementary figure 2 and table 1). Crosslinking efficiencies are expressed relative to +119 kb in CCR5 cells and normalised to mouse *Acta2* (see supplementary methods and supplementary figure 2) or to human *ACTA2* with similar results (supplementary figure 3a). Cohesin sites and the approximate positions of the *IFNG* and *IL26* genes are indicated (mean±SD, n=5 for CCR5 and CRTh2, n=4 for non-polarized CD4 T cells). *** p<0.005 (Student's T test, Th1 vs. non-polarized and Th1 vs. Th2).

b) 3D-FISH to determine nuclear diameters of CCR5$^+$ Th1 (red, 9.4+/−1.1 μm, n=50) and CRTh2$^+$ Th2 cells (black, 9.5+/−1.5 μm, n=50) and distances between *IFNG* alleles in individual CCR5 (red, 4.5+/−1.6 μm, n=50, minimum 1.5 μm) and CRTh2 cells (black, 5.0+/−1.9 μm, n=50, minimum 1.1 μm).

c) Long range interactions at *IFNG* in CCR5$^+$ Th1 cells occur prior to DNA replication. 3C analysis of *IFNG* in total CCR5$^+$ Th1 cells (red) compared to CCR5$^+$ Th1 cells in the G1 phase of the cell cycle (orange). Data are presented as in a), (mean±SE, n=2).

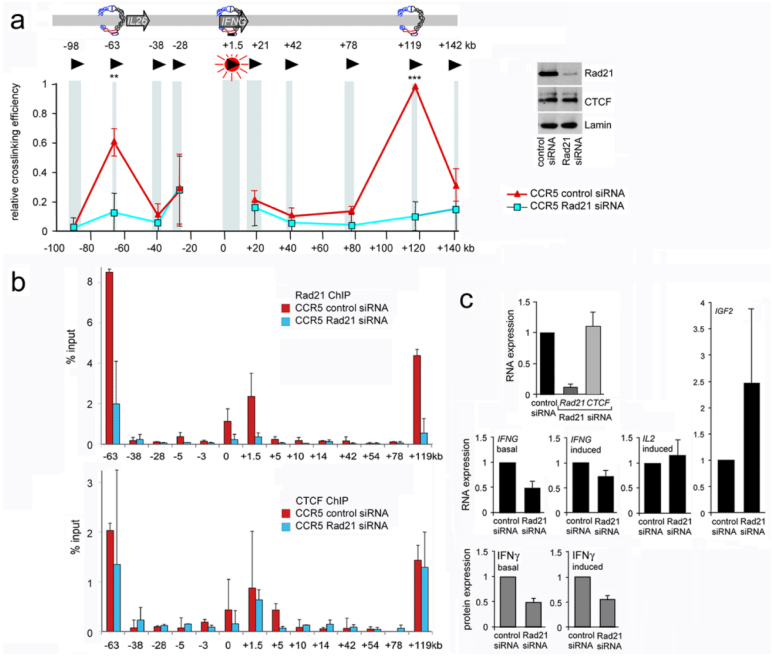

Figure 3. Long-range chromosomal interactions at *IFNG* require cohesin

a) CCR5$^+$ Th1 cells were transfected with control (red) or Rad21 (light blue) siRNA oligonucleotides. Long-range interactions at *IFNG* were assessed by 3C (mean±SE, n=4 for −63, −38 and +119kb, mean±SE, n=2 for −98, −28, +42, +78 and +142kb). Data are expressed relative to +119 kb in control siRNA treated CCR5$^+$ cells after normalisation to mouse *Acta2* in admixed mouse chromatin, which also served to control for technical aspects of the 3C methodology (supplementary figure 2). Normalisation to human *ACTA2* gave similar results (supplementary figure 3b). *** p<0.005, ** p<0.05 (Student's T test). The expression of CTCF and Rad21 was assessed by immunoblotting 72 hours after transfection of CCR5$^+$ Th1 cells with Rad21 or control siRNA. Lamin is a control.

b) ChIP for Rad21 (top) and CTCF (bottom) occupancy of *IFNG* 72 hours after transfection of CCR5$^+$ Th1 cells with control (red) or Rad21 siRNA (light blue). Primer positions are indicated in kb (mean± SE, n=2).

c) Real time RT-PCR analysis of CCR5$^+$ Th1 cells 72 hours after transfection with Rad21 siRNA or control siRNA. *Rad21* and *CTCF* are shown as knockdown controls (top panel, mean± SD, n=5). Levels of *IFNG* are shown one week (basal, mean± SD, n=5) or 4 hours after T cell activation (induced, mean± SD, n=4) with anti-CD3 and anti-CD28. *IL2* is shown as an activation control (mean± SD, n=3) and *IGF2* as known cohesin target (mean± SD, n=3). Data are normalised to *GAPDH, HPRT* and *TBP* and shown relative to control siRNA transfected CCR5 cells (middle panels). ELISA for basal (mean± SD, n=4) and activation-induced (mean± SD, n=4) IFNγ protein secretion. Data are shown relative to control siRNA CCR5 cells (bottom panels).

Europe PMC Funders Author Manuscripts